EPJ Web of Conferences **204**, 01011 (2019) https://doi.org/10.1051/epjconf/201920401011
Baldin ISHEPP XXIV

Overview of ALICE results on ultra-peripheral collisions

Evgeny Kryshen[1,*] on behalf of the ALICE Collaboration

[1]NRC "Kurchatov Institute", Petersburg Nuclear Physics Institute, Gatchina, Russia

Abstract. Lead nuclei, accelerated at the LHC, are sources of strong electromagnetic fields which can be used to measure photon-induced interactions in a new kinematic regime. These interactions can be studied in ultra-peripheral p–Pb and Pb–Pb collisions where impact parameters are larger than the sum of nuclear radii and hadronic interactions are strongly suppressed. Heavy quarkonium photoproduction is of particular interest since it is sensitive to gluon distributions in target hadrons. An overview of ALICE results on vector meson photoproduction in ultra-peripheral Pb–Pb and p–Pb collisions will be presented. Implications to study gluon density distributions and nuclear gluon shadowing will be discussed.

1 Introduction

Lead nuclei, accelerated at the LHC, are sources of strong electromagnetic fields, which are equivalent to a flux of quasi-real photons, thus Pb–Pb collisions can be used to measure $\gamma\gamma$, γp and γPb interactions in a new kinematic regime. These interactions are usually studied in ultra-peripheral collisions (UPC), characterized by impact parameters larger than the sum of the radii of the incoming hadrons, in which hadronic interactions are strongly suppressed [1, 2].

The ALICE detector perfectly matches all the requirements for UPC measurements. The UPC analysis strategy relies on the selection of events with only few tracks in an otherwise empty detector, therefore large pseudorapidity coverage is essential to guarantee the event emptiness. Almost continuous angular acceptance in ALICE is ensured with a central barrel covering the pseudorapidity range $|\eta| < 0.9$, a muon spectrometer in the forward direction ($-4 < \eta < -2.5$) and a set of forward detectors, the VZERO-A ($2.8 < \eta < 5.1$) and the VZERO-C ($-3.7 < \eta < -1.7$) used for triggering and multiplicity measurements. The Zero-Degree Calorimeters (ZDC), located at ± 114 m from the interaction point and covering $|\eta| > 8.8$, are used to detect neutrons from the electromagnetic dissociation or hadronic interactions of Pb nuclei. Since 2015, ALICE has been also equipped with ADA and ADC detectors covering very forward ($4.9 < \eta < 6.3$) and backward ($-7 < \eta < -4.8$) rapidity ranges. UPC events have been selected with dedicated triggers based on vetoes in the forward and backward directions and trigger inputs from the central barrel and the muon spectrometer. Further details on the ALICE experimental setup and performance can be found in [3, 4].

[*]e-mail: evgeny.kryshen@cern.ch

 https://doi.org/10.1051/epjconf/201920401011

2 Continuum dilepton photoproduction in Pb–Pb UPC

Continuum dilepton photoproduction is the simplest process that can be studied in ultra-peripheral Pb–Pb collisions at the LHC. In the equivalent photon approximation, its cross section can be expressed as a product of photon fluxes from Pb nuclei and $\gamma\gamma \rightarrow l^+l^-$ cross section that can be calculated in QED with high accuracy. ALICE results on the continuum dielectron photoproduction are shown in Fig. 1. ALICE, CMS and ATLAS results on dielectron and dimuon continuum photoproduction cross sections agree with leading order QED calculations over a wide range of invariant masses up to 100 GeV/c^2 [5–7] thus justifying the validity of the equivalent photon approximation and opening new opportunities to study other photon-induced processes in UPC.

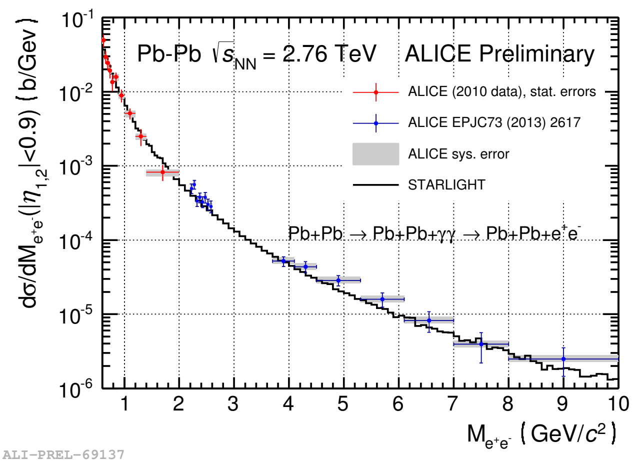

Figure 1. Continuum dielectron photoproduction cross section as function of dielectron invariant mass measured in Pb–Pb UPC at $\sqrt{s_{NN}}$ = 2.76 TeV by the ALICE collaboration [5] in comparison with leading order QED predictions from STARLIGHT [8]

3 J/ψ photoproduction in p–Pb UPC

Exclusive heavy quarkonium photoproduction is of particular interest for UPC studies since, in the leading order perturbative QCD, its cross section is proportional to the squared gluon density of the target [9]. ALICE acceptance in the LHC kinematics corresponds to Bjorken-x ranging from $x \sim 10^{-2}$ down to $x \sim 10^{-5}$, while the heavy-quark mass requires a virtuality Q^2 larger than a few GeV^2, hence introducing a hard scale.

Exclusive quarkonium photoproduction off protons in p–Pb UPC can be used to probe the poorly known behavior of the gluon density at low Bjorken-x down to 10^{-5} and search for gluon saturation effects. ALICE published two papers on the exclusive J/ψ photoproduction off protons in p–Pb UPC at $\sqrt{s_{\rm NN}}$ = 5.02 TeV [10, 11]. J/ψ mesons were detected via dilepton decays in three lepton detection options. In one case, the J/ψ candidate decays into a pair of leptons both of which are detected with the central-barrel detectors. The second case corresponds to a J/ψ candidate decaying into a pair of muons where one of them is measured with the muon spectrometer and the other with the central-barrel detectors. In the third case, both muons from J/ψ decays are detected in the muon spectrometer. Collisions were performed

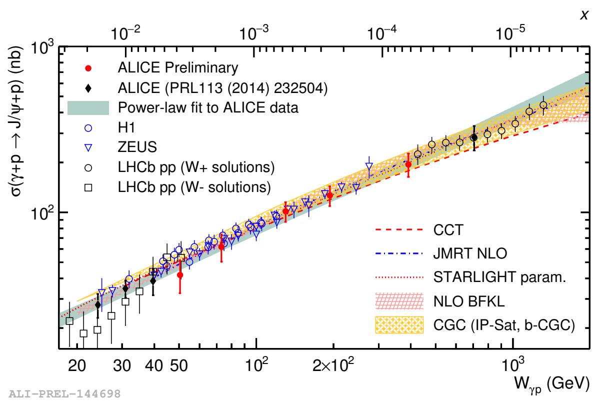

Figure 2. ALICE data on exclusive photoproduction of J/ψ off protons as a function of the center-of-mass energy of the photon-proton system in p–Pb collisions at $\sqrt{s_{NN}}$ = 5.02 TeV, compared to a power-law fit, to data from HERA, to the solutions from LHCb and to theoretical models

in two configurations by reversing the directions of the LHC beams thus allowing ALICE to probe forward and backward rapidities with a single arm muon spectrometer. Three lepton detection options and two beam configurations provided almost continuous coverage in the γp center-of-mass energy $W_{\gamma\mathrm{p}}$ from 20 to 700 GeV thus significantly extending the range probed at HERA. ALICE data on exclusive photoproduction of J/ψ off protons are shown in Fig. 2. The energy dependence of the photoproduction cross section is compatible with a power law showing no significant change in the gluon density power-law growth down to $x \sim 10^{-5}$ at $Q^2 \sim \frac{1}{4} m^2_{\mathrm{J}/\psi}$.

New data in p–Pb UPC collisions at $\sqrt{s_{\mathrm{NN}}}$ = 8.16 TeV were collected in 2016, as shown in Fig. 3. This sample will allow ALICE to extend the J/ψ photoproduction measurements to the TeV scale.

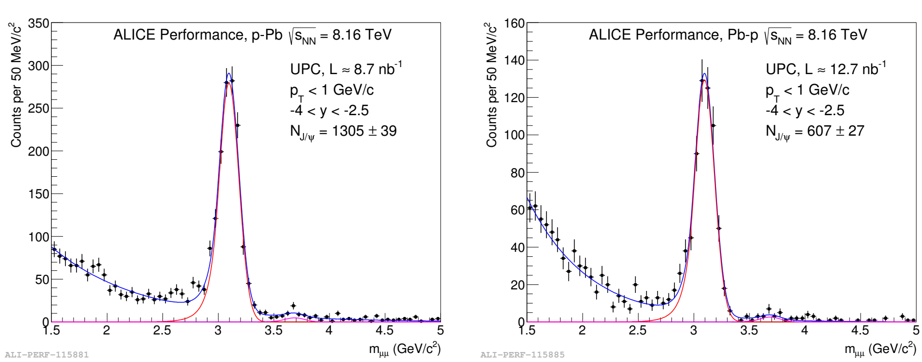

Figure 3. Invariant mass distributions for unlike-sign dimuons with pair $p_{\mathrm{T}} < 1$ GeV/c and rapidity $-4 < y < -2.5$ in ultra-peripheral p–Pb (left) and Pb-p (right) collisions at $\sqrt{s_{\mathrm{NN}}}$ = 8.16 TeV, corresponding to γp center-of-mass energy ranges $27 < W_{\gamma\mathrm{p}} < 57$ GeV and $700 < W_{\gamma\mathrm{p}} < 1480$ GeV respectively. J/ψ and ψ(2S) peaks are fitted with Crystal Ball functions on top of dimuon continuum fitted with an exponential function

4 Charmonium photoproduction in Pb–Pb UPC

Coherent quarkonium photoproduction in Pb–Pb UPC provides a direct tool to study nuclear gluon shadowing effects [12], which are poorly known and play a crucial role in the initial stages of heavy-ion collisions. First ALICE results from Run 1 on the coherent J/ψ photoproduction cross section in Pb–Pb UPC at $\sqrt{s_{\rm NN}}$ = 2.76 TeV are shown in Fig. 4, left [5, 13]. The measured cross section is in good agreement with the models based on the moderate gluon shadowing from the EPS09 global fit. ALICE data have been used to extract the gluon shadowing factor [12], see Fig. 4, right, indicating that coherent charmonium photoproduction in Pb–Pb UPC may serve as a promising tool to constrain gluon shadowing uncertainties.

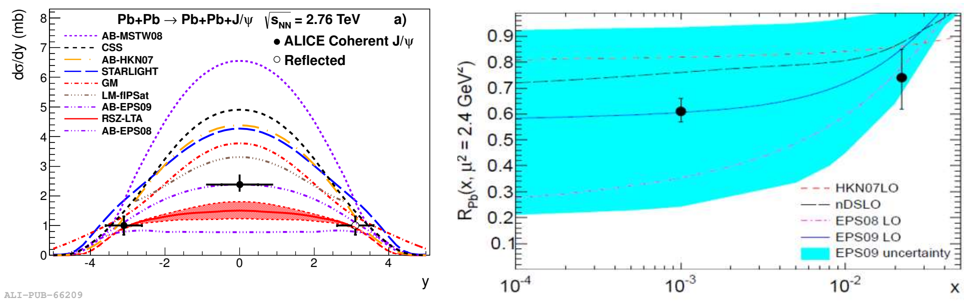

Figure 4. Left: coherent J/ψ photoproduction cross section in Pb–Pb UPC at $\sqrt{s_{\rm NN}}$ = 2.76 TeV measured by ALICE [5]. Right: Gluon shadowing factor extracted from the ALICE measurements [12]

ALICE also got first preliminary results on J/ψ photoproduction in Pb–Pb UPC at $\sqrt{s_{\rm NN}}$ = 5.02 TeV from Run 2. The obtained coherent J/ψ yield at forward rapidity is a factor 50 higher compared to Run 1 results [13] thanks to much higher integrated luminosity, improved trigger logic, a wider rapidity range and increased beam energy, see Fig. 5, left. The transverse momentum distribution for dimuons around the J/ψ mass includes several contributions as illustrated in Fig. 5, right. Coherent J/ψ photoproduction, when a photon interacts coherently with the whole nucleus, is characterized by a narrow transverse momentum distribution with $\langle p_{\rm T}\rangle \sim 60$ MeV/c. In the incoherent case the photon couples to a single nucleon. If the target nucleon stays intact, the charmonium $p_{\rm T}$ distribution is driven by the nucleon form factor, resulting in $\langle p_{\rm T}\rangle \sim 400$ MeV/c. J/ψ photoproduction on a single nucleon can be also accompanied by nucleon dissociation resulting in a high-$p_{\rm T}$ tail that was fitted with the H1 parameterization [14]. Contributions from continuum dimuon production and feed-down from ψ(2S) decays were also taken into account in the fits. The resulting coherent J/ψ photoproduction cross section at forward rapidity in ultra-peripheral Pb–Pb collisions at $\sqrt{s_{\rm NN}}$ = 5.02 TeV is compared to several theoretical predictions in Fig. 6. These results will help to constrain the nuclear gluon shadowing factor at $x \sim 10^{-2}$.

ALICE also collected a factor 5 higher statistics for J/ψ at central rapidity compared to Run 1 results. Invariant mass distributions for unlike-sign dimuons with pair $p_{\rm T} < 0.2$ GeV/c are shown in Fig. 7, left. The coherent J/ψ signal has been also observed in the $p\bar{p}$ channel, see Fig. 7, right. These mid-rapidity results will provide further constraints on the nuclear gluon shadowing at $x \sim 10^{-3}$.

ALICE also measured the coherent ψ(2S) cross section at mid-rapidity via the dilepton (l^+l^-) decay and in the channel $\psi(2S) \rightarrow J/\psi + \pi^+\pi^-$ followed by $J/\psi \rightarrow l^+l^-$ decay [15]. The measured coherent ψ(2S) photoproduction cross section, shown in Fig. 8 (right), disfavours the models without nuclear effects and those with strong gluon shadowing, however, different predictions rely on different reference $\gamma + \mathrm{p} \rightarrow \psi(2\mathrm{S}) + \mathrm{p}$ cross sections, thus preventing stronger conclusions. Many uncertainties on the measurement and on the $\gamma\mathrm{p}$ reference cancel in the ratio of the coherent $\psi(2\mathrm{S})$ and J/ψ cross sections. Surprisingly, the measured ratio $\sigma^{\mathrm{coh}}_{\psi(2\mathrm{S})}/\sigma^{\mathrm{coh}}_{\mathrm{J}/\psi} = 0.344^{+0.076}_{-0.074}$ appears to be a factor two larger than in $\gamma\mathrm{p}$ measurements at HERA [16] indicating that nuclear effects may differently affect 1S and 2S charmonium states. ALICE also measured a $\psi(2\mathrm{S})$ signal in $\psi(2\mathrm{S}) \rightarrow \mu^+\mu^-\pi^+\pi^-$ and $\psi(2\mathrm{S}) \rightarrow e^+e^-\pi^+\pi^-$ decay channels in Pb–Pb UPC at $\sqrt{s_{NN}} = 5.02$ TeV, as shown in Fig. 9. The experimental uncertainty of these measurements will be significantly improved with a much better statistics expected in Runs 3 and 4.

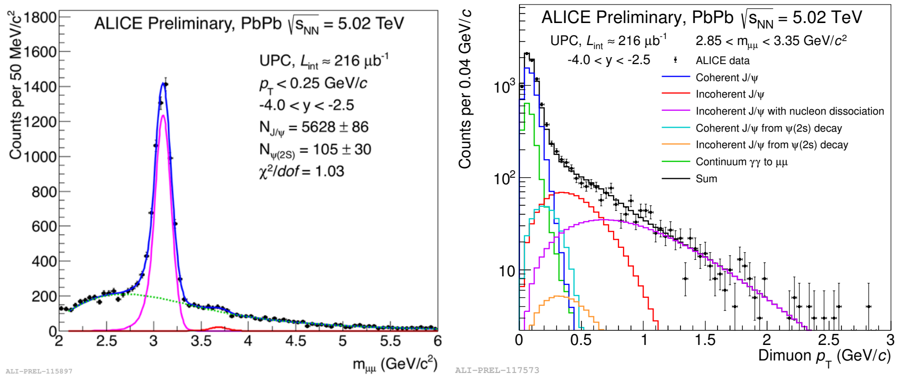

Figure 5. Left: invariant mass distribution for unlike-sign dimuons with pair $p_{\mathrm{T}} < 0.25$ GeV/c and rapidity $-4.0 < y < -2.5$ in ultra-peripheral Pb–Pb collisions at $\sqrt{s_{\mathrm{NN}}} = 5.02$ TeV. Right: transverse momentum distribution for unlike-sign dimuons around J/ψ mass fitted summing six different Monte Carlo templates produced using the STARLIGHT event generator [8]

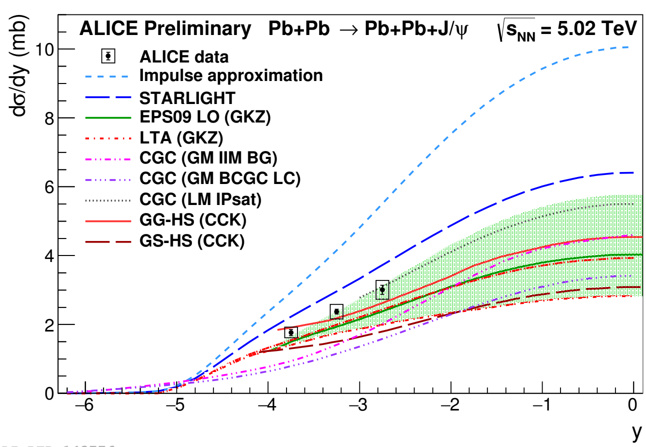

Figure 6. Measured coherent differential cross section of J/ψ photoproduction in ultra-peripheral Pb–Pb collisions at $\sqrt{s_{\mathrm{NN}}} = 5.02$ TeV. The error bars correspond to the statistical uncertainties, the open boxes to the systematic uncertainties. Results from various models are also shown

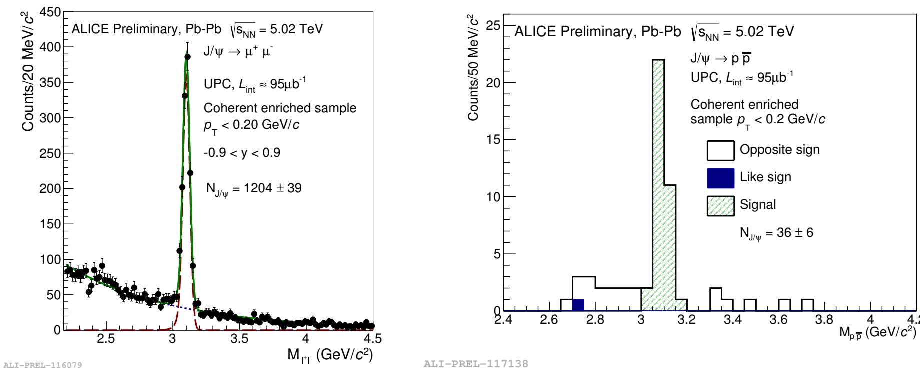

Figure 7. Invariant mass distribution for unlike-sign dimuons (left) and diprotons (right) with pair $p_T < 0.2$ GeV/c and rapidity $|y| < 0.9$ in ultra-peripheral Pb–Pb collisions at $\sqrt{s_{NN}} = 5.02$ TeV

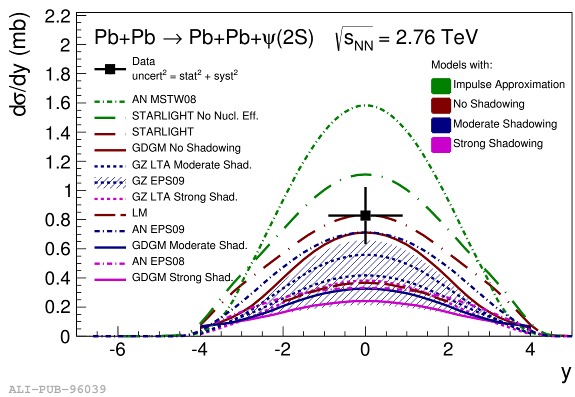

Figure 8. ALICE results on coherent $\psi(2S)$ photoproduction cross section in Pb–Pb collisions at $\sqrt{s_{NN}} = 2.76$ TeV in comparison with model predictions [15]

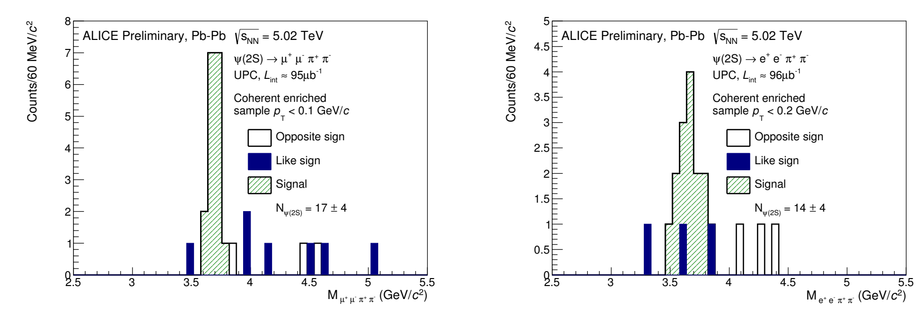

Figure 9. Invariant mass distributions for $\psi(2S) \to \mu^+\mu^-\pi^+\pi^-$ and $\psi(2S) \to e^+e^-\pi^+\pi^-$ decays collected by ALICE in Pb–Pb UPC at $\sqrt{s_{NN}} = 5.02$ TeV

5 Coherent ρ^0 photoproduction in Pb–Pb UPC

Coherent ρ^0 photoproduction measurements in ultra-peripheral collisions at the LHC are important for verification of ρ^0 photoproduction models [8, 17, 18] and investigation of nuclear shadowing effects in the nonperturbative regime [19]. ALICE has previously published results on coherent ρ^0 photoproduction in Pb–Pb UPC at $\sqrt{s_{NN}}$ = 2.76 TeV [20] showing good agreement with STARLIGHT predictions. The latest results on ρ^0 photoproduction at mid-rapidity in Pb–Pb UPC at $\sqrt{s_{NN}}$ = 5.02 TeV are presented in this section.

The two-pion transverse momentum distribution around the ρ^0 mass is shown in Fig. 10, left. It was fitted with STARLIGHT templates for coherent and incoherent ρ^0 photoproduction and contributions from dimuon continuum and uncorrelated like-sign background. The experimental transverse momentum distribution appears to be much narrower than the coherent template from STARLIGHT revealing the importance of impact-parameter-dependent nuclear effects [21].

Preliminary ALICE results on coherent differential cross section of ρ^0 photoproduction in Pb–Pb UPC at $\sqrt{s_{NN}}$ = 5.02 TeV are shown in Fig. 10, right, in comparison to several models. The GKZ model [17, 19] is based on the Glauber approach and takes into account photon inelastic diffraction into large masses resulting in sizable inelastic nuclear shadowing effects. The model has been found to agree with ALICE data on photoproduction in UPC at $\sqrt{s_{NN}}$ = 2.76 TeV [20], but slightly deviates from new ALICE measurements at $\sqrt{s_{NN}}$ = 5.02 TeV. The new ALICE data appear to be in agreement with STARLIGHT, which is also based on the Glauber formalism, but neglects the elastic part of the total ρN cross section and inelastic shadowing corrections [8]. The GM CDM model [18], based on the color-dipole approach and the Color Glass Condensate formalism, overestimates the data.

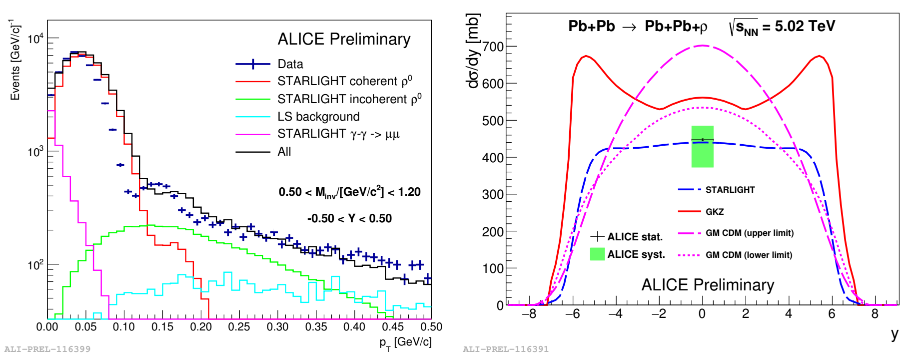

Figure 10. The two-pion transverse momentum distribution around the ρ^0 mass fitted with coherent and incoherent ρ^0 templates (left) and coherent differential cross section of ρ^0 photoproduction (right) measured by ALICE in ultra-peripheral Pb–Pb collisions at $\sqrt{s_{NN}}$ = 5.02 TeV

6 J/ψ photoproduction in peripheral Pb–Pb collisions

Although photon-induced reactions are typically measured in UPCs, they have also been observed in hadronic collisions of heavy ions. A strong excess in the yield of J/ψ at forward rapidities at very low transverse momenta $p_T < 0.3$ GeV/c, measured by ALICE in peripheral Pb–Pb collisions at $\sqrt{s_{NN}}$ = 2.76 TeV, results in a large nuclear modification factor $R_{AA} \sim 7$ in this p_T range, see Fig. 11 [22]. A similar excess has been also observed by ALICE for

J/ψ at central rapidity in peripheral Pb–Pb collisions at $\sqrt{s_{NN}}$ = 5.02 TeV, see Fig. 12. This excess is commonly interpreted as a signal of coherent J/ψ photoproduction off heavy-ion remnants, see e.g. [23, 24].

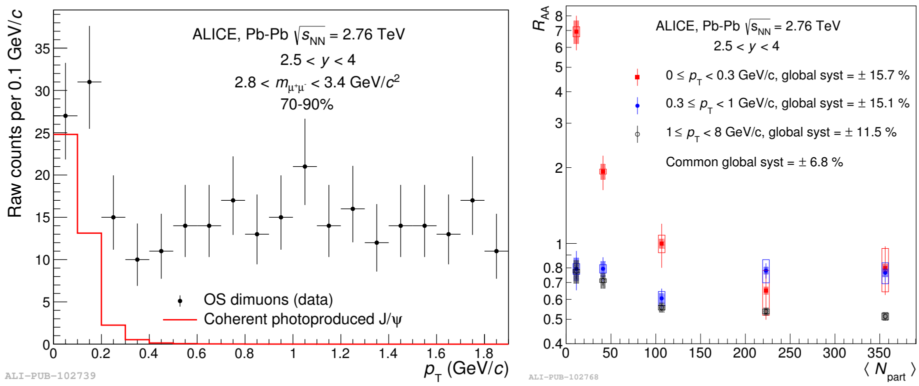

Figure 11. Left: transverse momentum spectrum for J/ψ at forward rapidity in peripheral Pb–Pb collisions at $\sqrt{s_{NN}}$ = 2.76 TeV. Right: J/ψ nuclear modification factor as function of the number of participants in different transverse momentum bins [22]

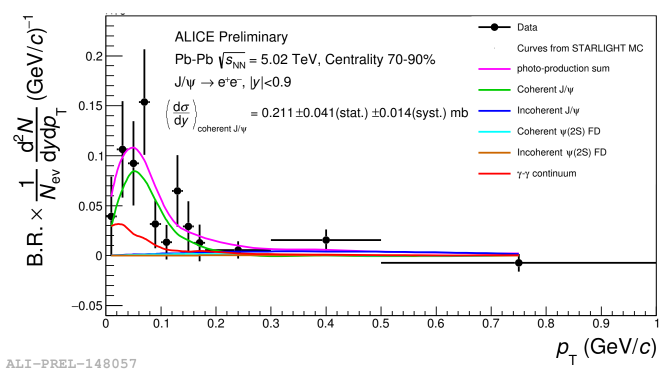

Figure 12. Transverse momentum spectrum for J/ψ at central rapidity in peripheral Pb–Pb collisions at $\sqrt{s_{NN}}$ = 5.02 TeV compared to several theoretical models

7 Conclusions

Vector meson photoproduction in ultra-peripheral collisions at the LHC has shown to be particularly useful as a probe of proton and nuclear structure. ALICE results on the exclusive J/ψ photoproduction off protons in p–Pb collisions indicate no significant change in the power-law x-dependence of the gluon density in the proton between HERA and LHC energies. ALICE results on the coherent J/ψ photoproduction in ultra-peripheral Pb–Pb collisions are in good agreement with models based on the moderate gluon shadowing from the EPS09 global fit. The measured ratio of coherent ψ(2S) and J/ψ photoproduction cross sections indicates that nuclear effects may affect differently 1S and 2S charmonium states. The latest

ALICE results on the coherent ρ^0 photoproduction in Pb–Pb collisions at $\sqrt{s_{NN}} = 5.02$ TeV lie below predictions based on the Gribov-Glauber formalism with inelastic shadowing corrections, but are in agreement with STARLIGHT where the elastic part of the total ρN cross section is neglected. Finally, ALICE has observed a surprising excess of J/ψ at low transverse momentum in peripheral Pb–Pb collisions that is commonly interpreted as a signal of coherent J/ψ photoproduction off heavy-ion remnants. The upcoming high-luminosity LHC era will bring much more precise measurements and hopefully new exciting discoveries in photon-induced physics.

References

[1] A.J. Baltz, Phys. Rept. **458**, 1 (2008). arXiv:0706.3356 [nucl-ex]
[2] J.G. Contreras, J.D. Tapia Takaki, Int. J. Mod. Phys. A **30**, 1542012 (2015)
[3] B.B. Abelev et al. (ALICE), Int. J. Mod. Phys. A **29**, 1430044 (2014). arXiv:1402.4476 [nucl-ex]
[4] K. Aamodt et al. (ALICE), JINST **3**, S08002 (2008)
[5] E. Abbas et al. (ALICE), Eur. Phys. J. C **73**, 2617 (2013). arXiv:1305.1467 [nucl-ex]
[6] CMS Collaboration, CMS-PAS-FSQ-16-012 (2018)
[7] The ATLAS Collaboration, ATLAS-CONF-2016-025 (2016)
[8] S.R. Klein, J. Nystrand, J. Seger, Y. Gorbunov, J. Butterworth, Comput. Phys. Commun. **212**, 258 (2017). arXiv:1607.03838 [hep-ph]
[9] M.G. Ryskin, Z. Phys. C **57**, 89 (1993)
[10] B.B. Abelev et al. (ALICE), Phys. Rev. Lett. **113**, 232504 (2014). arXiv:1406.7819 [nucl-ex]
[11] S. Acharya et al. (ALICE), arXiv:1809.03235 [nucl-ex] (2018)
[12] V. Guzey, E. Kryshen, M. Strikman, M. Zhalov, Phys. Lett. B **726**, 290 (2013). arXiv:1305.1724 [hep-ph]
[13] B. Abelev et al. (ALICE), Phys. Lett. B **718**, 1273 (2013). arXiv:1209.3715 [nucl-ex]
[14] C. Alexa et al. (H1), Eur. Phys. J. C **73**, 2466 (2013). arXiv:1304.5162 [hep-ex]
[15] J. Adam et al. (ALICE), Phys. Lett. B **751**, 358 (2015). arXiv:1508.05076 [nucl-ex]
[16] C. Adloff et al. (H1), Phys. Lett. B **541**, 251 (2002). arXiv:hep-ex/0205107
[17] V. Guzey, E. Kryshen, M. Zhalov, Phys. Rev. C **93**, 055206 (2016). arXiv:1602.01456 [nucl-th]
[18] V.P. Goncalves, M.V.T. Machado, Phys. Rev. C **80**, 054901 (2009). arXiv:0907.4123 [hep-ph]
[19] L. Frankfurt, V. Guzey, M. Strikman, M. Zhalov, Phys. Lett. B **752**, 51 (2016). arXiv:1506.07150 [hep-ph]
[20] J. Adam et al. (ALICE), JHEP **09**, 095 (2015). arXiv:1503.09177 [nucl-ex]
[21] V. Guzey, M. Strikman, M. Zhalov, Phys. Rev. C **95**, 025204 (2017). arXiv:1611.05471 [hep-ph]
[22] J. Adam et al. (ALICE), Phys. Rev. Lett. **116**, 222301 (2016). arXiv:1509.08802 [nucl-ex]
[23] J. Cepila, J.G. Contreras, M. Krelina, Phys. Rev. C **97**, 024901 (2018). arXiv:1711.01855 [hep-ph]
[24] W. Zha, S.R. Klein, R. Ma, L. Ruan, T. Todoroki, Z. Tang, Z. Xu, C. Yang, Q. Yang, S. Yang, Phys. Rev. C **97**, 044910 (2018). arXiv:1705.01460 [nucl-th]